Xue, W., Kitzing, T., Roessler, S., Zuber, J., Krasnitz, A., Schultz, N., Revill, K., Weissmueller, S., Rappaport, A.R., Simon, J., Zhang, J., Luo, W., Hicks, J., Zender, L., Wang, X.W., Powers, S., Wigler, M., Lowe, S.W.
A cluster of cooperating tumor-suppressor gene candidates in chromosomal deletions
(2012) Proceedings of the National Academy of Sciences of the United States of America, 109 (21), pp. 8212-8217.

A cluster of cooperating tumor suppressor gene candidates in chromosomal deletions

Wen Xue[a,b,1], Thomas Kitzing[a,1], Stephanie Roessler[c], Johannes Zuber[a], Alexander Krasnitz[a], Nikolaus Schultz[d], Kate Revill[a], Susann Weissmueller[a], Amy R. Rappaport[a], Janelle Simon[a,e], Jack Zhang[a], Weijun Luo[a], James Hicks[a], Lars Zender[a,f], Xin Wei Wang[c], Scott Powers[a], Michael Wigler[a,2], and Scott W. Lowe[a,e,2]

[a]Cold Spring Harbor Laboratory, Cold Spring Harbor, New York 11724, USA, [b]Current address: Koch Institute for Integrative Cancer Research and Department of Biology, Massachusetts Institute of Technology, Cambridge, MA 02139, USA, [c]Laboratory of Human Carcinogenesis, National Cancer Institute, National Institutes of Health, Bethesda, MD 20892, USA, [d]Computational Biology Center, Memorial Sloan-Kettering Cancer Center, New York, NY 10065, USA, [e]Howard Hughes Medical Institute, Cold Spring Harbor, NY 11724, USA, [f]Current address: Helmholtz Centre for Infection Research, 38124 Braunschweig, Germany and Department of Gastroenterology and Hepatology, Medical School Hannover, 30625 Hannover, Germany

The authors declare no potential conflict of interest.

Running title: Cooperating tumor suppressor genes on chromosome 8p

Classification: BIOLOGICAL SCIENCES/Genetics

Keywords: Chromosome 8p deletion, RNAi screen, Hepatocellular carcinoma, mouse cancer model, tumor suppressor genes

[1]These authors contributed equally to this work.

[2]Corresponding authors:

Scott W. Lowe, Ph.D.

Howard Hughes Medical Institute, Cold Spring Harbor Laboratory

1 Bungtown Road, Cold Spring Harbor, NY 11724

Phone: 516-367-8406; Email: lowe@cshl.edu

Mike Wigler, Ph.D.

Cold Spring Harbor Laboratory

1 Bungtown Road, Cold Spring Harbor, NY 11724

Phone: 516-367-8367; Email: wigler@cshl.edu

The large chromosomal deletions frequently observed in cancer genomes are often thought to arise as "second hit" mechanism in the process inactivating a tumor suppressor gene. Using a murine model system of hepatocellular carcinoma (HCC) and *in vivo* RNAi, we test an alternative hypothesis that such deletions can arise from selective pressure to attenuate the activity of multiple genes. By targeting the mouse orthologs of genes frequently deleted on human 8p22 and adjacent regions, which are lost in approximately half of several other major epithelial cancers, we provide evidence that multiple genes on chromosome 8p can cooperatively inhibit tumorigenesis in mice and show that their co-suppression can synergistically promote tumor growth. Additionally, in human HCC patients, the combined downregulation of functionally validated 8p tumor suppressors is associated with poor survival in contrast to the downregulation of any individual gene. Our data imply that large cancer-associated deletions can produce phenotypes distinct from those arising through loss of a single tumor suppressor gene and, as such, should be considered and studied as distinct mutational events.

Most cancer genomes contain large heterozygous deletions of uncertain biological significance. Early studies on the *RB* and *TP53* tumor suppressor genes suggested that such deletions can arise as one mechanism for loss of heterozygosity (LOH) and, consequently, it is often assumed they provide a "second hit" event to inactivate a single tumor suppressor gene (TSG) (1). However, genomic approaches have not conclusively identified a definitive TSG within some cancer-associated deletions, raising the possibility they occur through genomic instability or selection for the reduced activity of multiple genes. Even in chromosomal regions where a *bona fide* "two-hit" TSG has been identified, the large deletions often associated with loss of heterozygosity (LOH) reduce the dosage of neighboring genes that could, in principle, contribute to tumorigenesis in a haploinsufficient manner.

Large deletions encompassing regions of chromosome 8p are extremely common in human tumors (2, 3) and often occur together with 8q gains encompassing *MYC* (4). Previously, we validated the 8p gene *DLC1* – encoding a Rho GAP – as a tumor suppressor using a mouse model of hepatocellular carcinoma (HCC), confirming that its attenuation can serve as a driving oncogenic event (3). Although *DLC1* is at an epicenter of deletions, these deletions are frequently much larger and reduce the dosage of tens or hundreds of genes, often encompassing the entire 8p22 cytoband and beyond (2, 5, 6). Indeed, multiple candidate tumor suppressor genes have been proposed in the region (5-8). Here we explore the hypothesis that chromosome 8p deletions arise owing to selection for the attenuation of multiple genes.

Results

Chromosome 8p deletions are frequently large and co-occur with 8q gains and 17p loss. To better define regions affected by 8p deletions frequently occurring in human cancers, we determined the extent of chromosome 8p deletions from cancer genome datasets derived from array-based comparative genomic hybridization (aCGH) performed at Cold Spring

Harbor Laboratory and The Cancer Genome Atlas (TCGA) project totaling 1411 primary tumor samples and cell lines of HCC, breast, colon and lung cancer (Fig. 1*A* and Methods). These data show that approximately half of these tumors harbor heterozygous deletions of human chromosome 8p, often encompassing a large portion or the whole chromosome arm (Fig. 1*A*). Focusing on 8p deletions in HCC, we noticed that the most frequently deleted region on 8p centered around the *DLC1* gene (Fig. 1*A*) and in HCC occur more frequently than those on chromosome 17p encompassing *TP53* (3). However, this chromosome arm contains other candidate tumor suppressors (5-8) and, indeed, most deletions encompass regions adjacent to *DLC1*, including the whole 8p22 cytoband or even the whole chromosome 8p arm (Fig. 1*A*).

To identify a relevant genetic context to study 8p loss, we analyzed 197 primary HCCs (3, 9, 10) for copy number aberrations associated with 8p deletions (Fig. 1*B*). Amplifications of chromosome 1q, 5p, 6p and 8q (involving *MYC*), and loses including *TP53* on 17p significantly associate with 8p deletions (Fig.1*B*). Additionally, unsupervised hierarchical linkage clustering of 197 primary HCCs reveals that they fall within 12 groups and that the 8p loss, 8q gain and 17p loss cancers mainly cluster within one subgroup that represents ~40% of all HCCs (Fig. 1*C*). These data confirm that genotypes involving *MYC* overexpression and *TP53* loss are a valid genetic context in which to study candidate 8p tumor suppressors.

Chromosome 8p harbors multiple genes that inhibit tumorigenesis in mice. To identify tumor suppressors located on 8p, we tested whether RNAi-mediated suppression of various 8p genes would promote tumorigenesis in a mouse HCC model previously used for TSG discovery (11). Initially focusing in an unbiased approach on the 8p22 region surrounding *DLC1*, we transduced pools of 3 short hairpin RNAs (shRNAs) individually targeting each mouse ortholog of all 21 annotated 8p22 protein-coding genes into *p53-/-* liver progenitors overexpressing Myc – thereby approximating a relevant genetic context in human HCC progression. The resulting cell populations were then assessed for their tumorigenic potential

(Fig. 2*A*). While the parental cells transduced with a control shRNA were only weakly tumorigenic, cells harboring three of the 8p22 pools, including one containing shRNAs targeting Dlc1, substantially promoted tumorigenesis above background (Fig. 2*A*). The two other scoring shRNA pools targeted fibrinogen-like 1 (Fgl1), a secreted protein of the fibrinogen family that is a candidate TSG in human HCC (12), and vacuolar protein sorting 37 homolog a (Vps37a), a component of the ESCRT-I complex mediating endosome sorting whose under-expression is associated with poor survival in HCC patients (13).

Although chromosome 8p22 is at a deletion epicenter in HCC, most 8p deletions span even larger regions (Fig. 1*A*). We therefore questioned whether yet other tumor suppressor candidates lay in these adjacent regions. Since there were too many genes to test individually, we used selection criteria based on high deletion frequency, under-expression in human HCC, and potential tumor suppressive function according to the literature (Figs. S1, S2 and Table S1). We then repeated our experiments using shRNA pools targeting the mouse orthologs of 19 genes from 8p23 and 8p21-p11. Surprisingly, shRNAs targeting many of these genes (14 of 19) promoted tumorigenesis over background, although with substantial variability in tumor incidence and size (Fig. 2*B* and Table S2). Out of those, five showed a statistically significant increase over background at the time of tumor harvest (Fig. 2*B* and Table S2).

For further validation of the original candidates we subsequently tested the individual hairpins against the genes that showed significant tumor acceleration (*Fgl1*, *Vps37a*, *Arhgef10*, *Bin3*, *Bnip3l*, *Scara5*, *Trim35*) plus one more (*Fbxo25*) that, although not statistically significant yet yielded large tumors compared to control in a subset of mice (Table S2). Multiple shRNAs against Fgl1 or Vps37a that inhibited their corresponding targets promoted tumorigenesis in mice (Fig. 2*C* and Fig. S3). However, shRNA pools targeting Vps37a did not score consistently in all experiments, suggesting that it is a weak tumor suppressor or its action is susceptible to subtle variations in experimental conditions. For most hits examined (e.g. *Fbxo25*, *Fgl1* and

Trim35), the tumor promoting effect of single shRNAs correlated well with the observed level of knockdown (Fig. 2*C* and Fig. S3). However this was not always the case (e.g. Arhgef10), perhaps indicating that some of the scoring shRNAs suppress translation or that more complete gene suppression impacts an essential function, as we have described for *Rad17* (14).

In addition to *Fgl1* and *Vps37a*, among the novel genes with tumor suppressive function validated in this way were the autophagy regulator *Bnip3l* (15), the F-box protein encoding gene *Fbxo25* (16) and the ring finger, B-box, coiled-coil (RBCC) family gene *Trim35* (17), which has been recently reported as a novel HCC TSG candidate (18) (Fig. 2*C* and Fig. S3). Also validated in these experiments were the candidate TSGs *Scara5*, which negatively regulates focal adhesion kinase signaling (19) and *Arhgef10*, previously implicated in breast and urothelial carcinoma (5, 6) (Fig. S3). However, our screening assay was not without its limitations – for example, none of the single hairpins against *Bin3* accelerated tumorigenesis (data not shown). While this might indicate that the screening result was spurious, Bin3 shRNAs were also identified in a screen for tumor suppressors in lymphoma (20), and *Bin3* knockout mice are tumor prone (21). Regardless, most hits identified in the screen validated in follow up assays.

To control for the validity and specificity of our gene selection criteria and screening approach we repeated our experiments using shRNA pools targeting randomly selected genes on chromosome 8p in contrast to the selection criteria (Figs. S1, S2) we applied before to enrich for potential candidate genes. Contrary to the high frequency at which candidates scored in our initial assay (Fig. 2*B*), only 1 of 17 shRNA pools targeting randomly selected chromosome 8p genes promoted tumorigenesis above background (Fig. S4*A*). We also tested shRNA pools targeting genes corresponding to human 5q31, a frequently deleted region in acute myeloid leukemia but not in HCC. Only 1 of these 23 targets scored in our assay, and its suppression had only weak tumor-promoting effects (Fig S4*B*). The specificity of these results reinforces the

biological relevance of our selection criteria to enrich for genes with tumor suppressive function in our experimental system.

New tumor suppressors are apparently haploinsufficient. Several observations imply that most of the new genes we identified are relatively weak tumor suppressors that function through a haploinsufficient mode of action. Firstly, none of the new tumor suppressors were as potent as the well-established tumor suppressor gene, APC (see, for example, Fig. S3*A*). Secondly, none of the scoring shRNAs tested were capable of complete knockdown, and the resulting tumors retained residual mRNA levels (Fig. S3*B*). Lastly, and consistent with a report analyzing gene mutations of 8p21 genes (22), exon sequencing and methylation analysis of 13 matched tumor/normal HCC samples indicated that, while 9 tumors harbored 8p deletions, neither *DLC1* nor *FGL1* showed evidence of somatic mutation or promoter hypermethylation. Except for *ARHGEF10*, *DLC1* and *SCARA5* none of these genes show evidence of somatic point mutations in public databases (Table S3), and none approaching the frequency of 8p deletion. Thus, it seems unlikely that any of these biologically active tumor suppressors are subject to a two-hit mutational mechanism in HCC.

Individual 8p genes cooperate to suppress tumorigenesis. Our data imply that the impact of 8p deletions goes beyond the effects of *DLC1* mutation or, for that matter, the attenuation of any individual gene. To determine whether the co-attenuation of multiple genes with tumor suppressive function produced additive or cooperative effects, we examined the impact of co-attenuating *DLC1* – which is the only functionally validated 8p TSG in HCC (3) and at a deletion epicenter (Fig. 1*A*) – and the best validated other tumor suppressors from 8p22 (*Fgl1*) or adjacent regions (*Fbxo25* and *Trim35*). Indeed, co-attenuation of the 8p22 gene *Fgl1*, the 8p21 gene *Trim35*, or the 8p23 gene *Fbxo25* with *Dlc1* by co-transduction of shRNA vectors cooperated to promote tumor formation in mice (Fig. 3*A*). Consistently, co-suppression of the three scoring 8p22 genes (*Dlc1*, *Fgl1* and *Vps37a*) synergistically accelerated tumor growth

compared to single gene knockdown (Fig. 3*B,C*). In addition, copy number loss was highly correlated with *DLC1*, *TRIM35* and *FBXO25* mRNA underexpression in primary HCC and invasive breast cancer (Fig. S5), which is consistent with their co-deletion in most epithelial tumors (Fig. S5*A*,*B*, upper panels). Collectively these data imply that co-attenuation of physically linked tumor suppressor genes can cooperate during malignant transformation.

Downregulation of multiple 8p tumor suppressor genes predicts poor survival. To substantiate our findings in human cancer, we next asked if down-regulation of the validated individual 8p genes is associated with survival outcome in human HCC. We therefore analyzed gene expression data of a cohort of 195 HCC patients with available survival data (23, 24). While diminished expression of single genes or two genes together had no or only moderate association with survival outcome (Fig. 4*A,B*), diminished expression of all four validated cooperating TSGs (*DLC1, FGL1, FBXO25* and *TRIM35*) significantly correlated with poor survival (Fig. 4*C*) and thus might predict more aggressive disease progression. The reduced copy number status of each validated 8p gene (*DLC1*, *FGL1*, *TRIM35* and *FBXO25*) was significantly associated with survival (Fig. S6*A*), which is consistent with previous reports examining the collective impact of 8p loss on survival (4, 25) and the fact each is invariably co-deleted (Fig. S5A, upper panel). Together these data highlight that chromosome 8p contains multiple genes – likely more than identified here – whose attenuated activity can promote tumorigenesis (Fig. S6*B*). While each gene contributes modest effects, their combined attenuation may rival the impact of inactivating potent tumor suppressors such as *APC*, *RB* and *TP53*.

Discussion

Our data suggest that some recurrent cancer-associated deletions reflect the selective advantage of simultaneously targeting multiple “two hit” and/or haploinsufficient tumor suppressors (1). Such a situation has previously been described on chromosome 9p, though

has been largely attributed to the unique organization of the *INK4a/ARF* tumor suppressor locus (26). Nonetheless, in other *in vivo* RNAi screens we identified additional examples where multiple genes with tumor suppressive function could be validated within the same genomic region (11, 20) and further analysis of our HCC data reveals that large deletions surrounding well characterized TSG loci often encompass additional validated and/or candidate tumor suppressors (Fig. S7) supporting our idea that the biology mediated by these large deletions goes beyond the effects of individual genes.

The extent and complexity of chromosome 8p deletions suggests that various candidate tumor suppressor genes are targeted (5, 27, 28) and we have, for the first time, experimentally shown that co-suppression of linked 8p tumor suppressors promotes tumor formation more potently than any individual gene. Together with the frequency 8p deletions occur in most epithelial tumors we suggest that 8p deletions specifically arise from selective pressure to attenuate the activity of multiple genes that can be separated by large distances, which would explain the observed extent of the deletions at the copy number level. While it remains possible that genomic instability can fuel the loses we observe on chromosome 8p and in other genomic regions, our data imply these large events are selected for during tumor progression because of the presence of a discrete number of linked tumor suppressors whose complete or partial attenuation individually may have only a modest effect on tumor growth. This provides an important nuance to the two prevailing views that there is either one gene in the region that is the “driver” or that it is aneuploidy (chromosome imbalance) per se that is crucial. The frequent large deletions on other chromosomes (e.g. 3p, 5q, 9p and 17p) suggest that deletion of linked cancer genes may play a broad role in cancer phenotypes.

None of the tumor suppressor genes we functionally identify show evidence of somatic inactivation of the remaining allele at a frequency that approaches their deletion, suggesting that these genes do not fit the “canonical” view of a tumor suppressor as defined based on studies of

RB1 and *TP53*. Still, our functional data suggest that the expression of the 8p genes we identify is reduced in tumors with 8p deletions, and that the forced attenuation of these genes promotes malignant growth in an *in vivo* experimental system in a relevant cell type and genetic context. These results raise the possibility that large-scale genomic lesions can act through their effects on an opportunistic collection of linked genes rather than through disruption of a single resident gene. Given the extremely high frequency of these lesions in human cancers, this hypothesis warrants further investigation.

Although this study addresses the origin of large somatic deletions occurring in human tumors, the notion that copy number alterations may frequently target multiple drivers likely extends to oncogenes located in common regions of amplification as well. Hence, work from our group and others has functionally validated multiple drivers in common amplicons that, in some cases, cooperate to produce more aggressive features and contribute to the maintenance of disease (29-32). Collectively, these data raise the possibility that methods integrating the complexity of copy number aberrations in tumors may be more accurate in predicting and delineating tumor behavior than methods that focus on individual genes (33, 34).

Whether there is a biological rationale underlying the physical linkage of some TSGs and how their molecular function synergizes is not clear. However, the fact that these genes can cooperate to suppress tumorigenesis implies that concomitant loss of multiple genes may create unexpected vulnerabilities not easily revealed through the study of single genes. Hence, co-deletion of the 8p TSGs may not only create dependency on Rho signaling (3), but might also deregulate autophagy (15), ubiquitination (16) and other processes. While the relevant biological effects remain to be determined and are the focus of ongoing work, our results demonstrate that cancer-associated deletions can create phenotypes unique from those arising through loss of a single tumor suppressor gene, and should be considered and studied as distinct mutational events.

Materials and Methods

Genomic data analysis. We analyzed aCGH data produced using representational oligonucleotide microarray analysis (ROMA) for the frequency and size of deletions in a series of human HCC, breast, colon and lung cancers available at Cold Spring Harbor Laboratory (3, 11, 33). We utilized this method to study gene-dosage alterations in human HCC as recently described (33). Copy number aberrations (CNAs) were visualized from the individual ROMA aCGH plots of the specific HCC samples using the Integrated Genomics Viewer (IGV) software (Broad Institute, http://www.broadinstitute.org/igv/home). Additionally, available CNA from SNP6 arrays from The Cancer Genome Atlas (http://cancergenome.nih.gov/) for HCC, breast, colon and lung adenocarcinoma were visualized using IGV software and analyzed for occurrence of chromosome 8p deletion.

Co-occurrence of gene deletions and amplifications in HCC was performed as described (34) by analyzing the aCGH dataset available at Cold Spring Harbor Laboratory combined with two previously reported HCC aCGH datasets (9, 10) publicly available at the Gene Expression Omnibus (GEO; www.ncbi.nlm.nih.gov/geo) with accession numbers GSE19399 and GSE9845, totaling 197 primary HCCs and 12 HCC cell lines. Briefly, statistical significant CNAs in HCC were analyzed for frequency and co-occurrence in individual samples and Fisher's Exact test was used to calculate p-values for co-occurrence with chromosome 8p deletion.

Hierarchical clustering was performed by analyzing the combined HCC dataset (see above) using Nexus Copy Number™ software 5.1 (BioDiscovery), adding the significant CNAs as individual factors for each sample and using the complete linkage hierarchical cluster tool to group the samples based on the overall genomic aberrations. Subsequently, the annotated significant CNAs for individual samples were highlighted to visualize their occurrence within the

clusters. Additionally, Nexus Copy Number™ software 5.1 (BioDiscovery) was used to determine deletion frequencies of the 8p genes outside of 8p22 (Supplementary Table S1).

Gene expression analysis was performed using Oncomine database (www.oncomine.org) comparing multiple available HCC gene expression datasets. Comparison of copy number aberration to gene expression was based on available TCGA datasets for HCC (53 samples) and invasive breast cancer (320 samples). Cancer genome datasets and bioinformatic tools to visualize different parameters for analysis of genomic data are accessible through the MSKCC cBio Core homepage (www.cbioportal.org).

shRNA design, cloning and vector construction. miR30-shRNAs targeting murine orthologs of human 8p genes [which shows synteny to mouse chromosomes 8A4-B2 (human 8p22), 8A1 (human 8p23) and 14D1 (8p21)] were designed as previously described (35). miR30 design shRNAs were PCR amplified from 97-mer oligonucleotides and cloned into MSCV-miR30-SV40-GFP (MLS) or MSCV-miR30-PGK-Puromycin-IRES-GFP (MLP) retroviral vectors (36) and sequence verified. Myc was expressed using MSCV retroviral vectors (11). For double cooperativity experiments shRNAs were subcloned into MSCV-miR30-PGK-Neo-GFP (LMNG) or MSCV-miR30-PGK-Neo-mCherry (LMNR).

Generation of liver carcinomas and tumor imaging. Isolation, culture and retroviral infection of murine hepatoblasts were described recently (32, 37). Liver progenitor cells from ED=18 p53-/- fetal livers were immortalized with MSCV based retroviruses expressing Myc–IRES-GFP or Myc-IRES-Luciferase (11). For generating liver carcinomas, $2x10^6$ ED=13.5 liver progenitors were retrovirally transduced and transplanted into livers of female C57/B6 (6-8 weeks of age) by intrasplenic injection or injected subcutaneously into NCR nu/nu mice. As controls hairpins targeting Renilla or an unspecific shRNA against human pRb were used. Validation of single hairpin experiments (see Supplementary Figure S3) were performed in

newly derived liver progenitor cells from ED=18 p53-/- fetal livers immortalized with MSCV based retroviruses expressing Myc.

For double cooperativity experiments liver carcinomas were generated using liver progenitor cells immortalized with MSCV-based retroviruses expressing Myc by retroviral co-transduction of the two shRNAs in MSCV-based vectors containing either GFP or mCherry and subsequent subcutaneous injection of $1x10^6$ cells into NCR nu/nu mice. The following shRNAs were used: shRen.713, shDlc1.3163, shTrim35.3034, shFbxo25.1551 and shFgl1.560. Triple infection knockdown experiments were performed accordingly, except that 3x control virus was used and single shRNA virus was mixed with 2x control virus to achieve comparable virus titers among the samples. Cells were injected either subcutaneously or intrasplenicly. Tumor volume of subcutaneous tumors were calculated based on caliper measurements by the modified ellipsoidal formula: $0.5x(\text{length} \times \text{width}^2)$. To address tumor penetrance the number of tumors per injected site was counted and is shown in Supplementary Table S2.

Intrasplenic injections and bioluminescence imaging for triple knockdown experiments were performed as described recently (37-39).

Gene expression and survival analysis from human samples. The gene expression data of the HCC cohort has been published earlier (23, 24). Briefly, gene expression profiling was carried out using NCI's Human Array-Ready Oligo Set microarray platform and Affymetrix GeneChip HG-U133A 2.0 arrays, respectively. The microarray data are publicly available at the Gene Expression Omnibus (GEO; www.ncbi.nlm.nih.gov/geo) with accession numbers GSE5975 and GSE14520. The gene expression of DLC1 and FGL1 was obtained from the Affymetrix arrays. TRIM35 and FBXO25 were not available on the Affymetrix platform and therefore the gene expression data of NCI's Human Array-Ready Oligo Set microarray was used. Gene expression of 195 patients was available on both microarray platforms and for 192

patients, survival data as well as cause of death were available. Statistical analysis was performed as described (24).

Tissue culture and qRT-PCR. Retroviral-mediated gene transfer was performed using Phoenix packaging cells (G. Nolan, Stanford University, Stanford, CA) as described (40). RNA purification and qRT-PCR were performed as described (3). qRT-PCR reactions were done in triplicates using gene-specific primers. The expression level of each gene was normalized to β-actin or Gapdh. qRT-PCR primers were designed using PrimerBank (http://pga.mgh.harvard.edu/primerbank/) and listed in the Supplementary Information (Table S4).

Acknowledgements

We thank B. Ma, A. Shroff and S. Muller for excellent technical assistance. We are grateful to Z. Xuan for his help on statistics, to L. Dow and M. Saborowski for critically reading the manuscript. We thank all members of the Lowe laboratory for critical discussions throughout the course of the study. T.K. is a recipient of a DFG Postdoctoral Fellowship (KI1605/1-1). W.X. is a recipient of an AACR Centennial Predoctoral Fellowship, J. Zuber is a Seligson clinical fellow, and S.W.L. is a Howard Hughes Medical Institute Investigator. This work was supported by a program project grant from the National Cancer Institute, a Cancer Target Discovery and Development consortium grant, and the Don Monti Memorial Research Foundation. M. Wigler's support for this work comes from the Dept. of the Army W81XWH04-1-0477; The Breast Cancer Research Foundation; M.W. is an American Cancer Society Research Professor.

Author contributions

W.X. and T.K. performed experiments and analyzed results. S.R. and X.W.W. analyzed

and contributed human tumor data. J. Zuber, S.W. and A.R. designed RNAi reagents. A.K., N.S., T.K., J. Zhang, M.W., J.H., and S.P. analyzed CGH data. S.P. and K.R. examined DNA methylation. W.X., T.K., J. Zuber, L.Z., M.W. and S.W.L. designed the study and wrote the manuscript.

References

1. Baker SJ*, et al.* (1989) Chromosome 17 deletions and p53 gene mutations in colorectal carcinomas. *Science* 244(4901):217-221.
2. Birnbaum D*, et al.* (2003) Chromosome arm 8p and cancer: a fragile hypothesis. *Lancet Oncol* 4(10):639-642.
3. Xue W*, et al.* (2008) DLC1 is a chromosome 8p tumor suppressor whose loss promotes hepatocellular carcinoma. *Genes Dev* 22(11):1439-1444.
4. El Gammal AT*, et al.* (2010) Chromosome 8p deletions and 8q gains are associated with tumor progression and poor prognosis in prostate cancer. *Clinical cancer research : an official journal of the American Association for Cancer Research* 16(1):56-64.
5. Cooke SL*, et al.* (2008) High-resolution array CGH clarifies events occurring on 8p in carcinogenesis. *BMC Cancer* 8:288.
6. Williams SV*, et al.* (2010) High-resolution analysis of genomic alteration on chromosome arm 8p in urothelial carcinoma. *Genes, chromosomes & cancer* 49(7):642-659.
7. Berger AH*, et al.* (2010) Identification of DOK genes as lung tumor suppressors. *Nature genetics* 42(3):216-223.
8. Gorringe KL*, et al.* (2009) Are there any more ovarian tumor suppressor genes? A new perspective using ultra high-resolution copy number and loss of heterozygosity analysis. *Genes Chromosomes Cancer* 48(10):931-942.
9. Beroukhim R*, et al.* (2010) The landscape of somatic copy-number alteration across human cancers. *Nature* 463(7283):899-905.
10. Chiang DY*, et al.* (2008) Focal gains of VEGFA and molecular classification of hepatocellular carcinoma. *Cancer Res* 68(16):6779-6788.
11. Zender L*, et al.* (2008) An oncogenomics-based in vivo RNAi screen identifies tumor suppressors in liver cancer. *Cell* 135(5):852-864.

12. Yu HT*, et al.* (2009) Specific expression and regulation of hepassocin in the liver and down-regulation of the correlation of HNF1alpha with decreased levels of hepassocin in human hepatocellular carcinoma. *J Biol Chem* 284(20):13335-13347.

13. Lai MW*, et al.* (2009) Expression of the HCRP1 mRNA in HCC as an independent predictor of disease-free survival after surgical resection. *Hepatol Res* 39(2):164-176.

14. Bric A*, et al.* (2009) Functional identification of tumor-suppressor genes through an in vivo RNA interference screen in a mouse lymphoma model. *Cancer Cell* 16(4):324-335.

15. Zhang J & Ney PA (2009) Role of BNIP3 and NIX in cell death, autophagy, and mitophagy. *Cell Death Differ* 16(7):939-946.

16. Hagens O, Minina E, Schweiger S, Ropers HH, & Kalscheuer V (2006) Characterization of FBX25, encoding a novel brain-expressed F-box protein. *Biochim Biophys Acta* 1760(1):110-118.

17. Kimura F*, et al.* (2003) Cloning and characterization of a novel RING-B-box-coiled-coil protein with apoptotic function. *J Biol Chem* 278(27):25046-25054.

18. Jia D*, et al.* (2011) Genome-wide copy number analyses identified novel cancer genes in hepatocellular carcinoma. *Hepatology* 54(4):1227-1236.

19. Huang J*, et al.* (2010) Genetic and epigenetic silencing of SCARA5 may contribute to human hepatocellular carcinoma by activating FAK signaling. *The Journal of clinical investigation* 120(1):223-241.

20. Scuoppo C*, et al.* (in Press) A tumor suppressor network relying on the polyamine-hypusine axis. *Nature*.

21. Ramalingam A*, et al.* (2008) Bin3 deletion causes cataracts and increased susceptibility to lymphoma during aging. *Cancer research* 68(6):1683-1690.

22. Mourra N*, et al.* (2008) High-resolution genotyping of chromosome 8 in colon adenocarcinomas reveals recurrent break point but no gene mutation in the 8p21 region. *Diagn Mol Pathol* 17(2):90-93.

23. Jia HL*, et al.* (2007) Gene expression profiling reveals potential biomarkers of human hepatocellular carcinoma. *Clin Cancer Res* 13(4):1133-1139.

24. Roessler S*, et al.* (2010) A unique metastasis gene signature enables prediction of tumor relapse in early-stage hepatocellular carcinoma patients. *Cancer research* 70(24):10202-10212.

25. Ren N*, et al.* (2006) The prognostic value of circulating plasma DNA level and its allelic imbalance on chromosome 8p in patients with hepatocellular carcinoma. *J Cancer Res Clin Oncol* 132(6):399-407.

26. Krimpenfort P*, et al.* (2007) p15Ink4b is a critical tumour suppressor in the absence of p16Ink4a. *Nature* 448(7156):943-946.

27. Pole JC*, et al.* (2006) High-resolution analysis of chromosome rearrangements on 8p in breast, colon and pancreatic cancer reveals a complex pattern of loss, gain and translocation. *Oncogene* 25(41):5693-5706.

28. Roessler S*, et al.* (2011) Integrative Genomic Identification of Genes on 8p Associated With Hepatocellular Carcinoma Progression and Patient Survival. *Gastroenterology*.

29. Guan Y*, et al.* (2007) Amplification of PVT1 contributes to the pathophysiology of ovarian and breast cancer. *Clinical cancer research : an official journal of the American Association for Cancer Research* 13(19):5745-5755.

30. Kendall J*, et al.* (2007) Oncogenic cooperation and coamplification of developmental transcription factor genes in lung cancer. *Proc Natl Acad Sci U S A* 104(42):16663-16668.

31. Sawey ET*, et al.* (2011) Identification of a therapeutic strategy targeting amplified FGF19 in liver cancer by Oncogenomic screening. *Cancer Cell* 19(3):347-358.

32. Zender L*, et al.* (2006) Identification and validation of oncogenes in liver cancer using an integrative oncogenomic approach. *Cell* 125(7):1253-1267.

33. Hicks J*, et al.* (2006) Novel patterns of genome rearrangement and their association with survival in breast cancer. *Genome Res* 16(12):1465-1479.

34. Taylor BS*, et al.* (2010) Integrative genomic profiling of human prostate cancer. *Cancer Cell* 18(1):11-22.

35. Zuber J*, et al.* (2011) Toolkit for evaluating genes required for proliferation and survival using tetracycline-regulated RNAi. *Nature biotechnology* 29(1):79-83.

36. Dickins RA*, et al.* (2005) Probing tumor phenotypes using stable and regulated synthetic microRNA precursors. *Nat Genet* 37(11):1289-1295.

37. Zender L*, et al.* (2005) Generation and analysis of genetically defined liver carcinomas derived from bipotential liver progenitors. *Cold Spring Harb Symp Quant Biol* 70:251-261.

38. Xue W*, et al.* (2007) Senescence and tumour clearance is triggered by p53 restoration in murine liver carcinomas. *Nature* 445(7128):656-660.

39. Zuber J*, et al.* (2009) Mouse models of human AML accurately predict chemotherapy response. *Genes Dev* 23(7):877-889.

40. Schmitt CA*, et al.* (2002) Dissecting p53 tumor suppressor functions in vivo. *Cancer Cell* 1(3):289-298.

Figure legends

Fig. 1. Chromosome 8p deletion characteristics and co-occurring genomic aberrations. (*A*) Depiction of size and extent of chromosome 8p deletions (blue – deletion; dark blue indicating homozygous and light blue indicating heterozygous deletions; red – amplification) from individual HCCs, breast cancer, colon cancer and lung adenocarcinoma based on aCGH data analysis (see Methods). The 8p22 cytoband is highlighted with a dashed line with the organization of the 8p22 genes indicated on the right. (*B*) Chromosome 8p deletions co-occur with genomic aberrations in HCC including amplifications (red) of 1q, 5p, 6p and 8q and deletions (blue) of 17p. Fisher's exact test was used for statistical calculations. (*C*) Unsupervised hierarchical clustering of genomic aberrations indicates twelve groups within the HCC dataset (n=197). Occurrence of 8p deletion (dark red), 8q amplification (dark blue) and 17p deletions (dark orange) within the individual samples is highlighted below the dendrogram.

Fig. 2. Chromosome 8p deletions target multiple tumor suppressors. (*A*,*B*) Average volume of tumors derived from subcutaneously injected *p53-/-;Myc* immortalized liver cells infected with indicated shRNA pools. Error bars denote S.D. (n=6). Student´s t-test comparing normalized samples at the time when mice were sacrificed relative to control was used for statistical calculations. (*C*) Average tumor volumes of subcutaneously injected *p53-/-;Myc* immortalized liver cells infected with indicated individual shRNAs. Error bars denote S.D. (n=8). Student´s t-test comparing normalized samples at day 42 relative to control was used to calculate p-values.

Fig. 3. Cooperativity of 8p tumor suppressors. (*A*) Average tumor volumes (n=4) of subcutaneously injected *p53-/-;Myc* immortalized liver cells infected or co-infected with indicated shRNAs. As controls hairpins targeting Renilla were used. Error bars denote S.D. Significance was calculated using Student´s t-test comparing normalized samples at day 35 relative to control. (*B*) Average tumor volumes of subcutaneously injected *p53-/-;Myc* immortalized liver

cells infected with indicated single shRNAs or co-infected with all three shRNAs (Fgl1, Vps37a and Dlc1). Error bars denote S.D. (n=4). Of note, owing to the experimental organization the individual contribution of each tumor suppressor genes in the triple gene knockdown could not be determined. (*C*) Representative bioluminescence images from 5 mice with *in situ* liver tumors from intrasplenically injected *p53-/-;Myc* immortalized liver cells infected with indicated single shRNAs or triple infected with Fgl1, Vps37a and Dlc1. Numbers shown indicate mean intensities of luciferase signals +/- S.D. (n=5).

Fig. 4. Survial association with 8p gene expression in HCC patients. Survival curves of HCC patients comparing high vs. low expression of indicated single genes (*A*) or indicated gene combinations of 2 genes (*B*). (*C*) Survival association of liver cancer patients (n=192) for the entire cohort (all patients, black line) versus combined low (red line) or high expression (blue line) of DLC1, FGL1, TRIM35 and FBXO25 (4 genes). Statistical tests were performed as described (24).

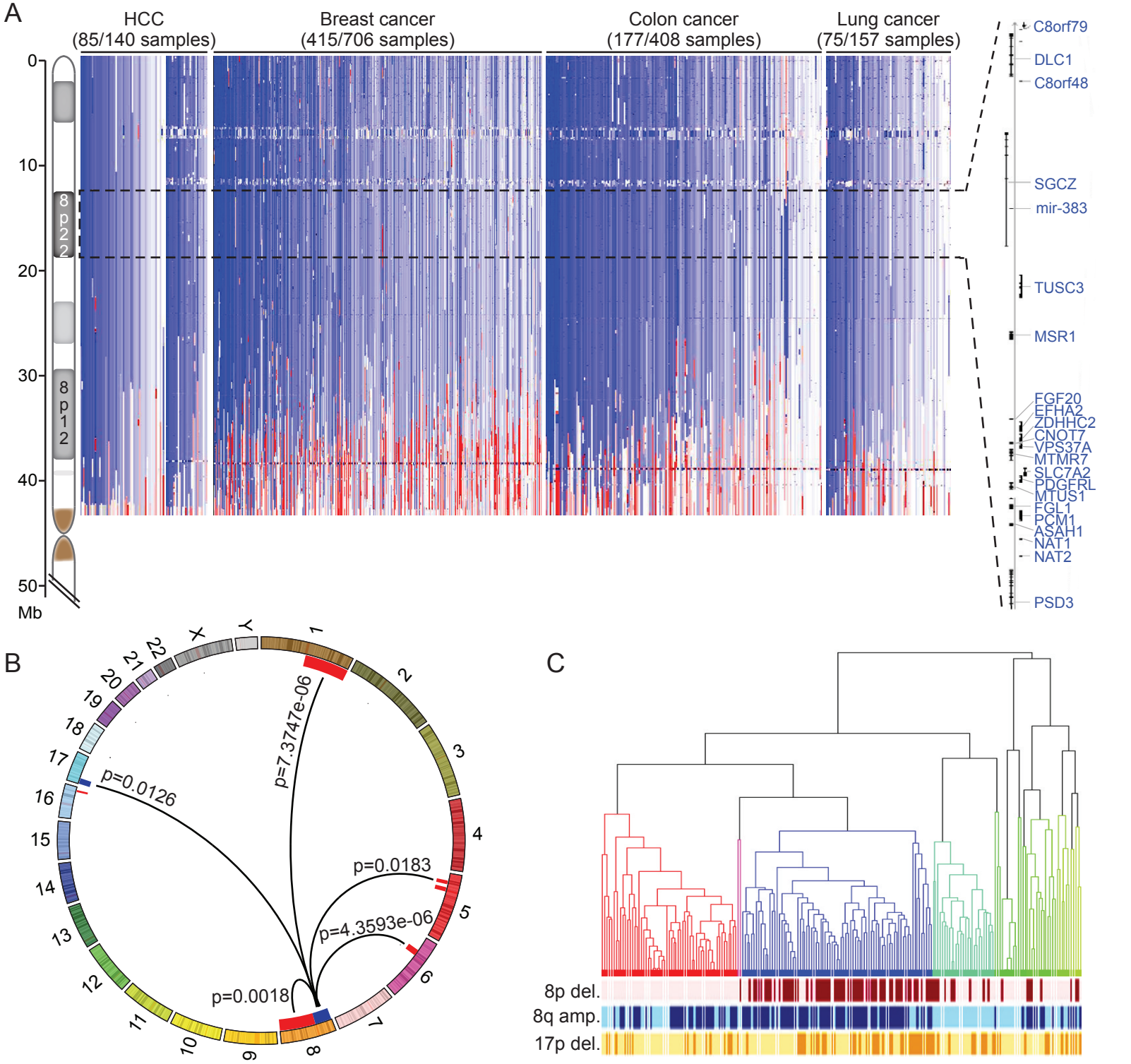
A
HCC
(85/140 samples)
Breast cancer
(415/706 samples)
Colon cancer
(177/408 samples)
Lung cancer
(75/157 samples)
0
10
20
30
40
50
Mb
8p22
8p12
C8orf79
DLC1
C8orf48
SGCZ
mir-383
TUSC3
MSR1
FGF20
EFHA2
ZDHHC2
CNOT7
VPS37A
MTMR7
SLC7A2
PDGFRL
MTUS1
FGL1
PCM1
ASAH1
NAT1
NAT2
PSD3
B
p=7.3747e-06
p=0.0126
p=0.0183
p=4.3593e-06
p=0.0018
C
8p del.
8q amp.
17p del.

Figure 1

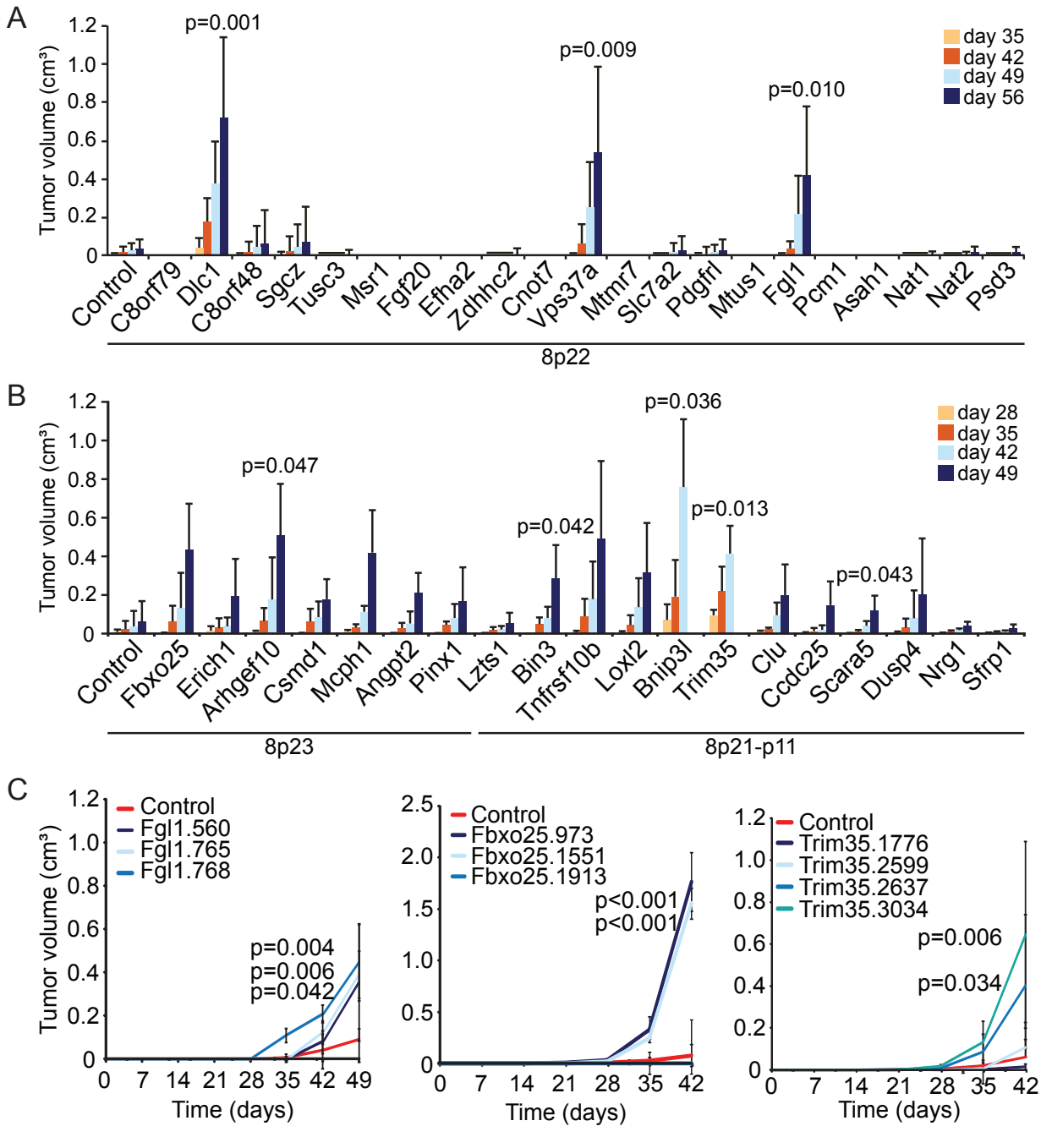
A
Tumor volume (cm³)
p=0.001
p=0.009
p=0.010
day 35
day 42
day 49
day 56
Control
C8orf79
Dlc1
C8orf48
Sgcz
Tusc3
Msr1
Fgf20
Efha2
Zdhhc2
Cnot7
Vps37a
Mtmr7
Slc7a2
Pdgfrl
Mtus1
Fgl1
Pcm1
Asah1
Nat1
Nat2
Psd3
8p22
B
Tumor volume (cm³)
p=0.047
p=0.042
p=0.036
p=0.013
p=0.043
day 28
day 35
day 42
day 49
Control
Fbxo25
Erich1
Arhgef10
Csmd1
Mcph1
Angpt2
Pinx1
Lzts1
Bin3
Tnfrsf10b
Loxl2
Bnip3l
Trim35
Clu
Ccdc25
Scara5
Dusp4
Nrg1
Sfrp1
8p23
8p21-p11
C
Tumor volume (cm³)
Control
Fgl1.560
Fgl1.765
Fgl1.768
p=0.004
p=0.006
p=0.042
Time (days)
Control
Fbxo25.973
Fbxo25.1551
Fbxo25.1913
p<0.001
p<0.001
Time (days)
Control
Trim35.1776
Trim35.2599
Trim35.2637
Trim35.3034
p=0.006
p=0.034
Time (days)

Figure 2

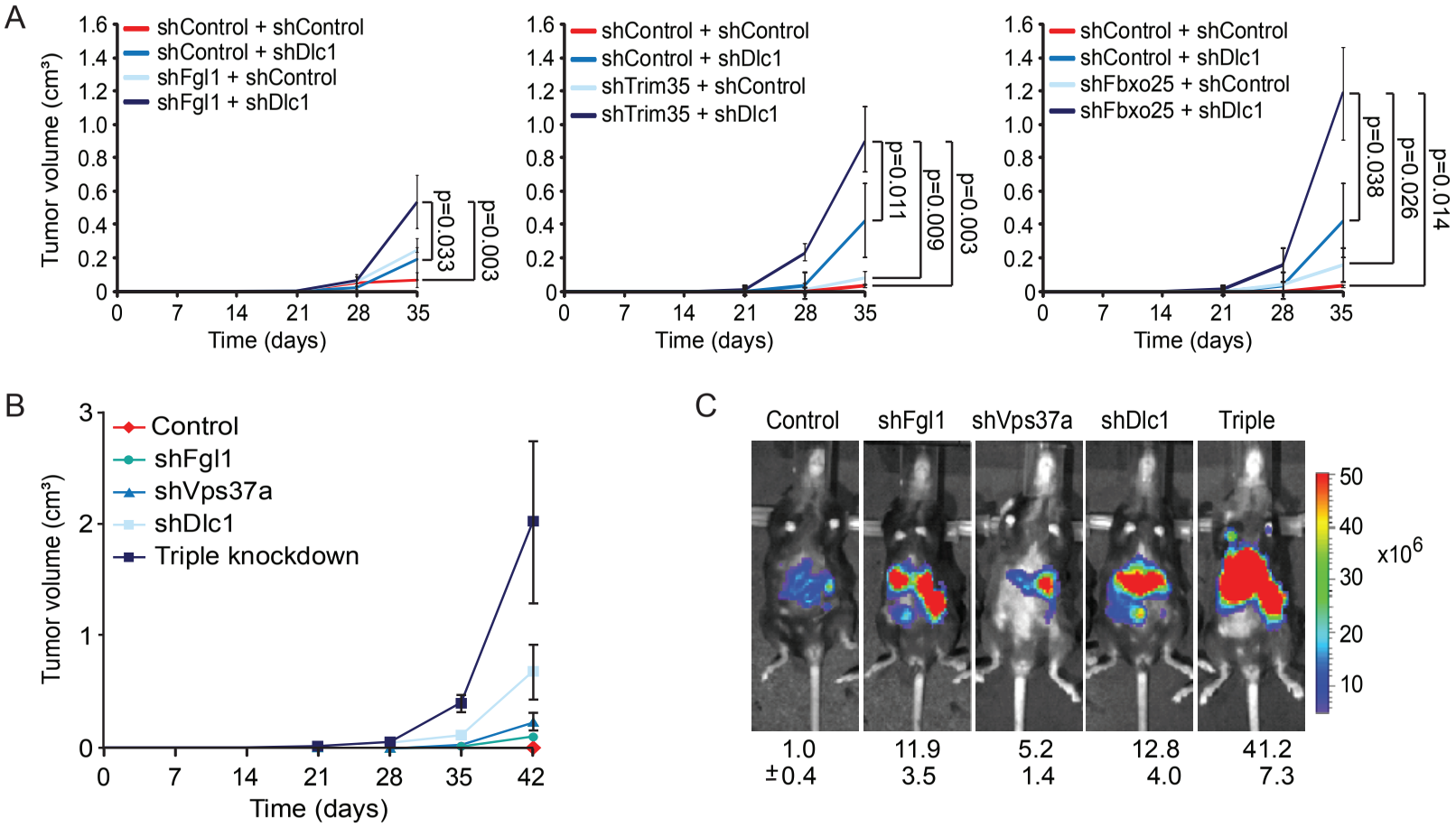
A
shControl + shControl
shControl + shDlc1
shFgl1 + shControl
shFgl1 + shDlc1
Tumor volume (cm³)
Time (days)
p=0.033
p=0.003
shControl + shControl
shControl + shDlc1
shTrim35 + shControl
shTrim35 + shDlc1
p=0.011
p=0.009
p=0.003
shControl + shControl
shControl + shDlc1
shFbxo25 + shControl
shFbxo25 + shDlc1
p=0.038
p=0.026
p=0.014
B
Control
shFgl1
shVps37a
shDlc1
Triple knockdown
Tumor volume (cm³)
Time (days)
C
Control
shFgl1
shVps37a
shDlc1
Triple
x10^6
1.0 ±0.4
11.9 3.5
5.2 1.4
12.8 4.0
41.2 7.3

Figure 3

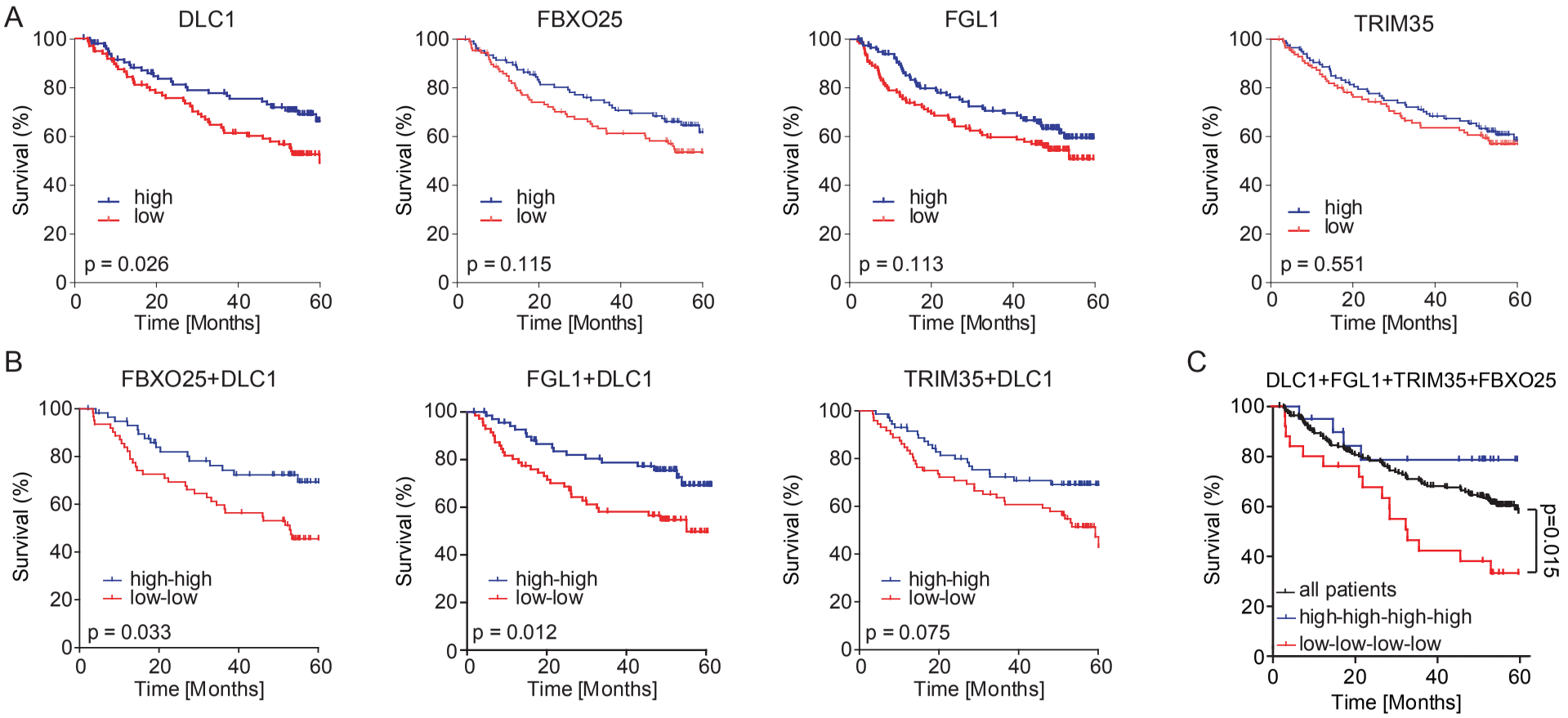
A
DLC1
FBXO25
FGL1
TRIM35
Survival (%)
Time [Months]
high
low
p = 0.026
p = 0.115
p = 0.113
p = 0.551
B
FBXO25+DLC1
FGL1+DLC1
TRIM35+DLC1
high-high
low-low
p = 0.033
p = 0.012
p = 0.075
C
DLC1+FGL1+TRIM35+FBXO25
p=0.015
all patients
high-high-high-high
low-low-low-low

Figure 4

SUPPLEMENTARY INFORMATION FOR:

A cluster of cooperating tumor suppressor gene candidates in chromosomal deletions

Wen Xue[a,b,1], Thomas Kitzing[a,1], Stephanie Roessler[c], Johannes Zuber[a], Alexander Krasnitz[a], Nikolaus Schultz[d], Kate Revill[a], Susann Weissmueller[a], Amy R. Rappaport[a], Janelle Simon[a,e], Jack Zhang[a], Weijun Luo[a], James Hicks[a], Lars Zender[a,f], Xin Wei Wang[c], Scott Powers[a], Michael Wigler[a,2], and Scott W. Lowe[a,e,2]

[a]Cold Spring Harbor Laboratory, Cold Spring Harbor, New York 11724, USA, [b]Current address: Koch Institute for Integrative Cancer Research and Department of Biology, Massachusetts Institute of Technology, Cambridge, MA 02139, USA, [c]Laboratory of Human Carcinogenesis, National Cancer Institute, National Institutes of Health, Bethesda, MD 20892, USA, [d]Computational Biology Center, Memorial Sloan-Kettering Cancer Center, New York, NY 10065, USA, [e]Howard Hughes Medical Institute, Cold Spring Harbor, NY 11724, USA, [f]Current address: Helmholtz Centre for Infection Research, 38124 Braunschweig, Germany and Department of Gastroenterology and Hepatology, Medical School Hannover, 30625 Hannover, Germany

[1]These authors contributed equally to this work.

[2]To whom correspondence may be addressed. E-mail: lowe@cshl.edu or wigler@cshl.edu

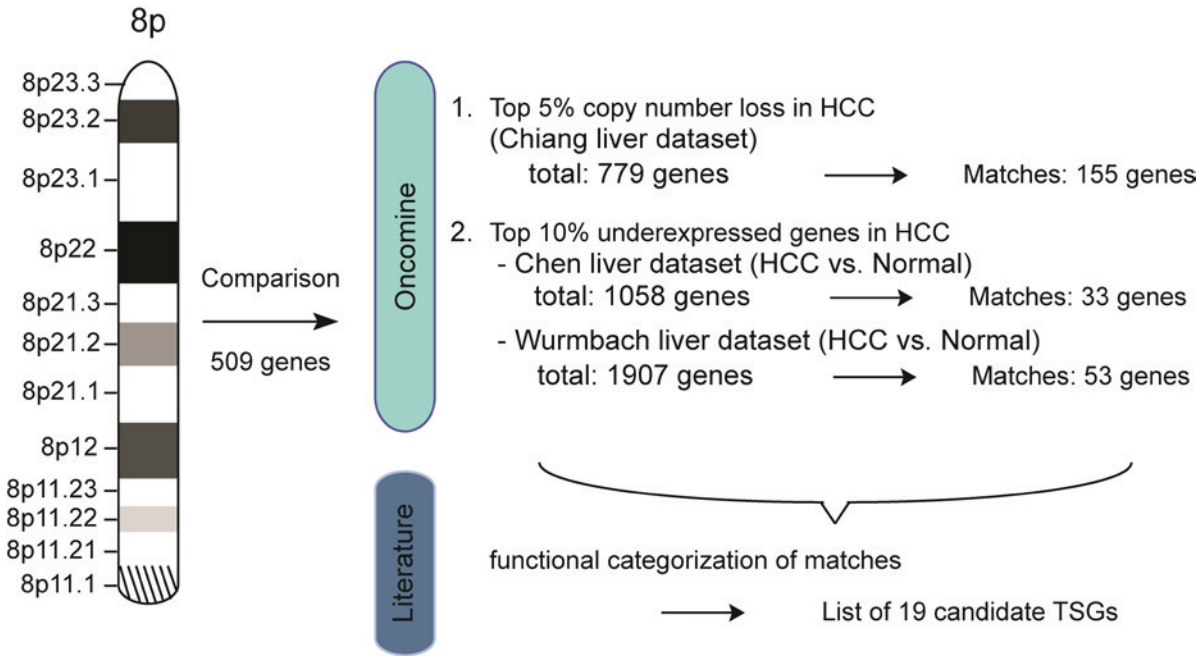

Fig. S1. Selection criteria for chromosome 8p candidate tumor suppressor genes. Schematic outline of the criteria for selection of 8p candidate tumor suppressors. For full gene list and chromosome location see Supplementary Table S1.

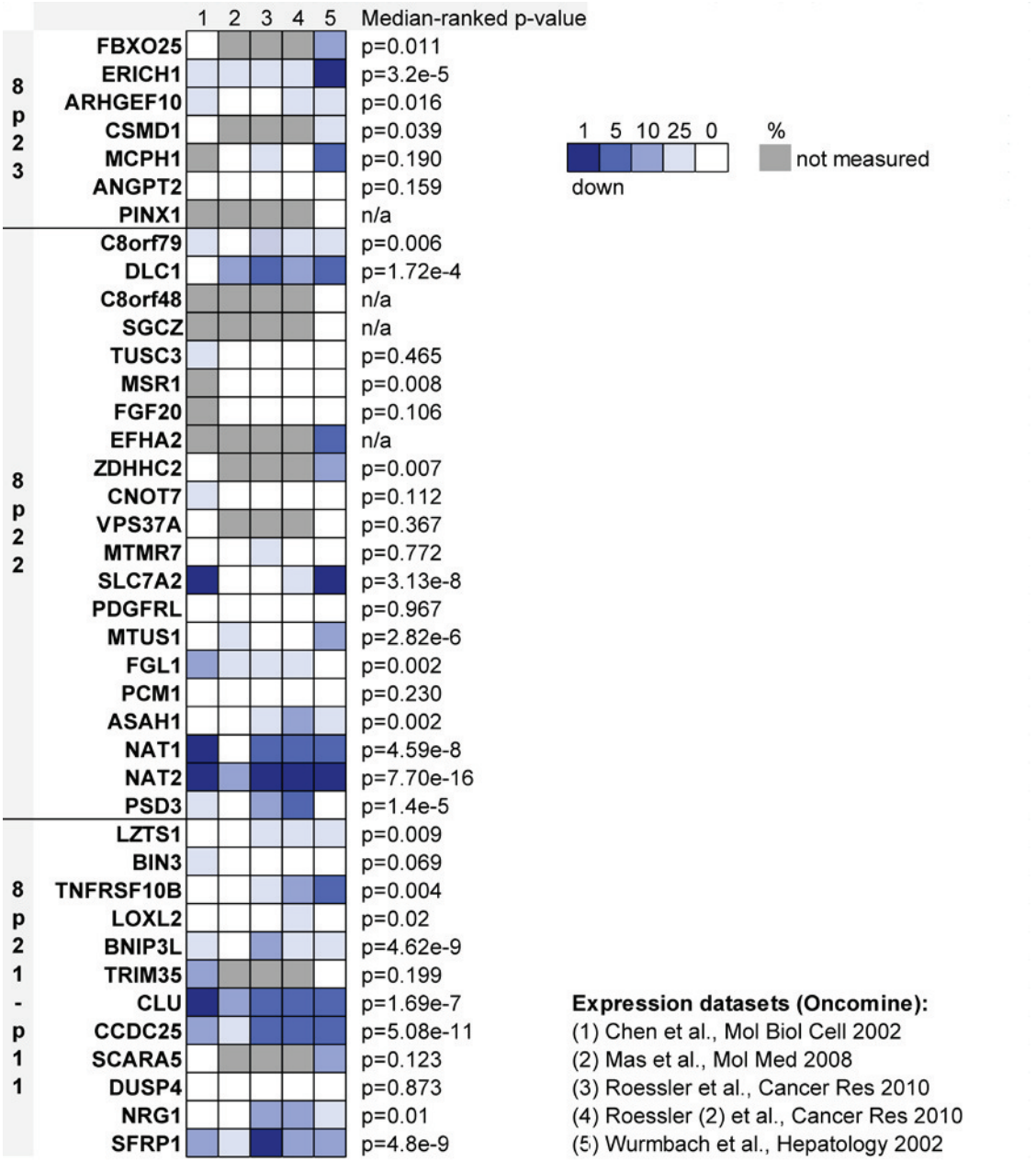

Fig. S2. Gene expression of 8p genes selected for RNAi screening across multiple datasets comparing hepatocellular carcinoma (HCC) to normal liver. Oncomine database (oncomine.org) was used to analyze gene expression across multiple datasets comparing HCC to normal (1-4). p-value is the median-ranked p-value across the different datasets.

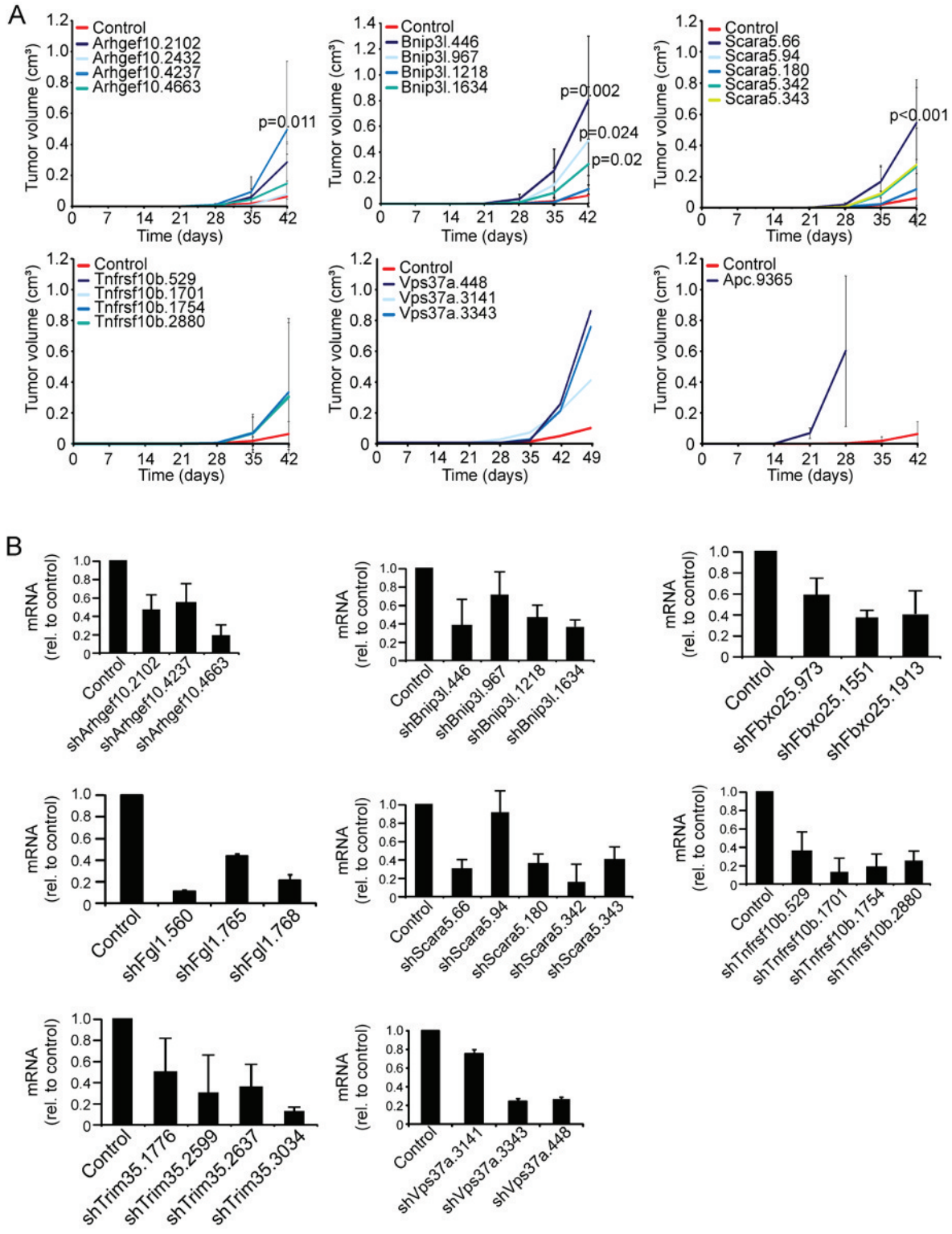

Fig. S3. Functional validation of individual shRNAs targeting chromosome 8p genes. (*A*) Average tumor volumes of subcutaneously injected *p53-/-;Myc* immortalized liver cells infected with indicated individual shRNAs used in the pooled screening (Fig. 2*A*,*B*). Error bars denote S.D.

(n=8). Student´s t-test comparing normalized samples at day 42 relative to control was used to calculate p-values. Apc was used as positive control. (*B*) qRT-PCR of *p53-/-;Myc* immortalized liver cells infected with indicated individual shRNAs used for injections in (*A*). Error bars denote S.D.

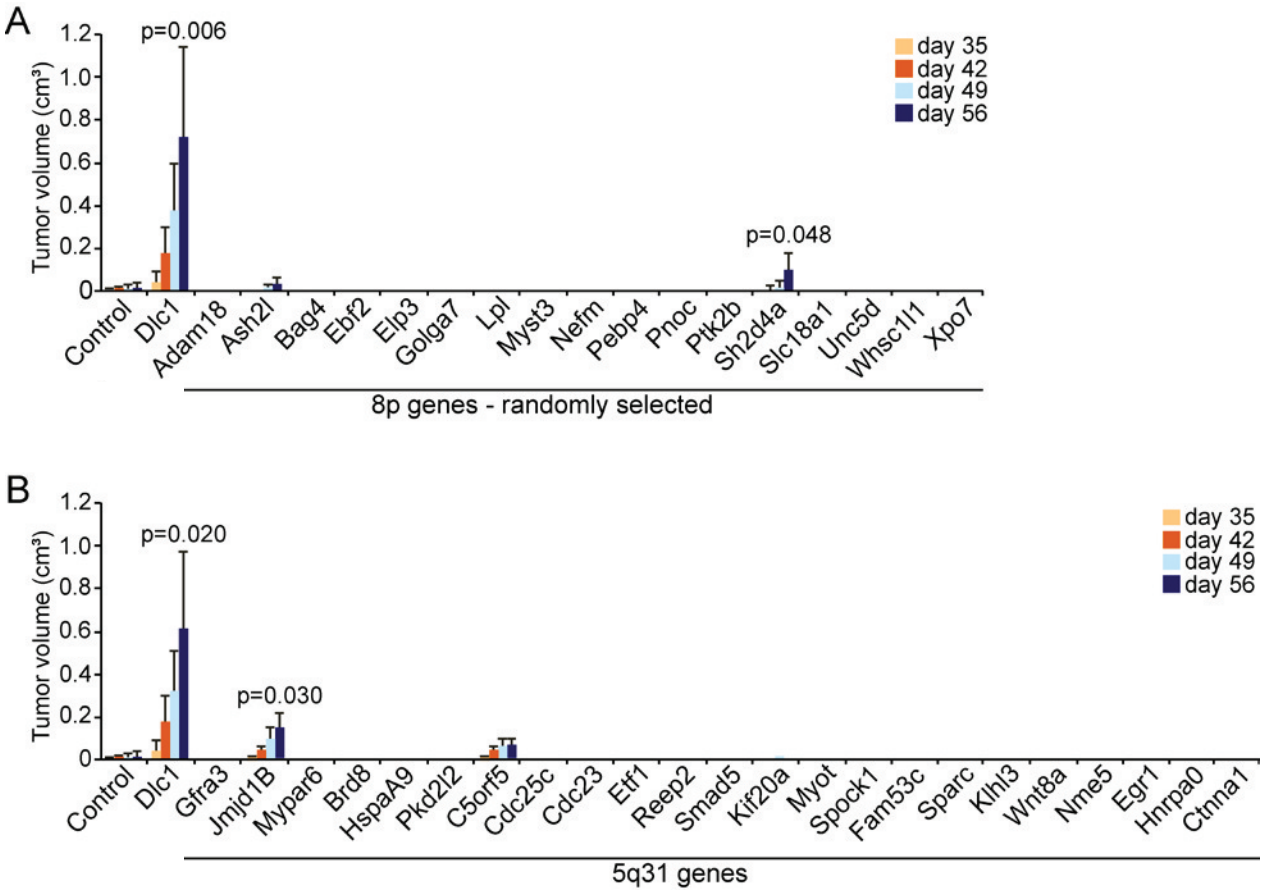

Fig. S4. Control *in vivo* RNAi screen for randomly selected 8p genes and 5q31 genes. (*A-B*) Average tumor volumes of subcutaneously injected *p53-/-;Myc* immortalized liver cells infected with shRNA pools targeting indicated 8p genes or 5q31 genes, respectively. Error bars denote S.D. (n=4). Student´s t-test comparing normalized samples at day 56 relative to control was used for statistical calulations.

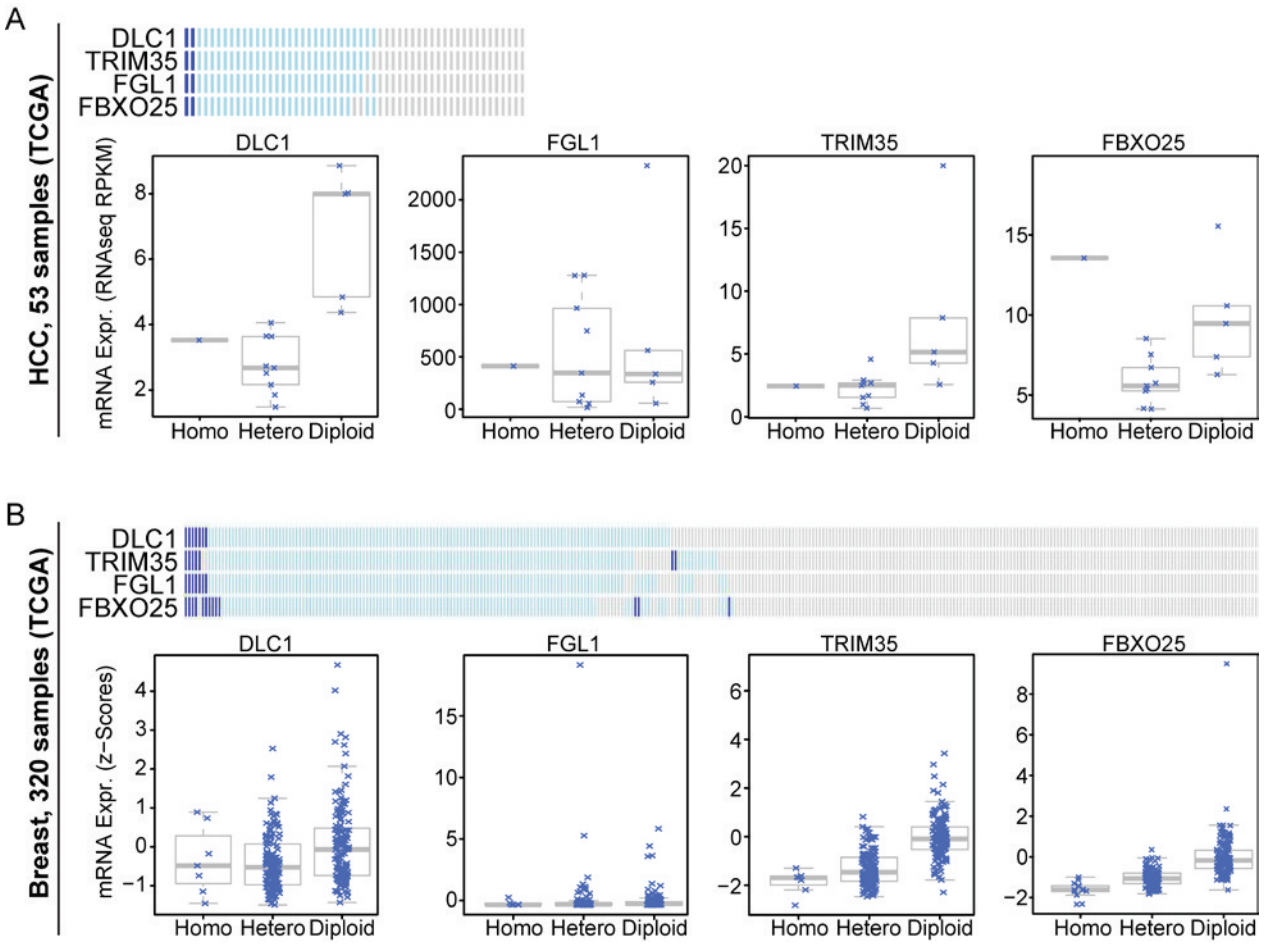

Fig. S5. Comparison of copy number loss to gene expression. Putative copy number events based on GISTIC algorithm for DLC1, TRIM35, FGL1 and FBXO25 in each individual sample are shown (*A*,*B* upper panels) with dark blue indicating homozygous loss and light blue indicating heterozygous loss. Of note, “homozygous” samples can also be tetraploid tumors with only one remaining 8p arm. Gene expression compared to copy number (GISTIC) for the indicated genes are shown in the lower panels for HCC (*A*) and invasive breast cancer (*B*). Data analysis is based on available TCGA data processed by the MSKCC cBio Core (www.cbioportal.org).

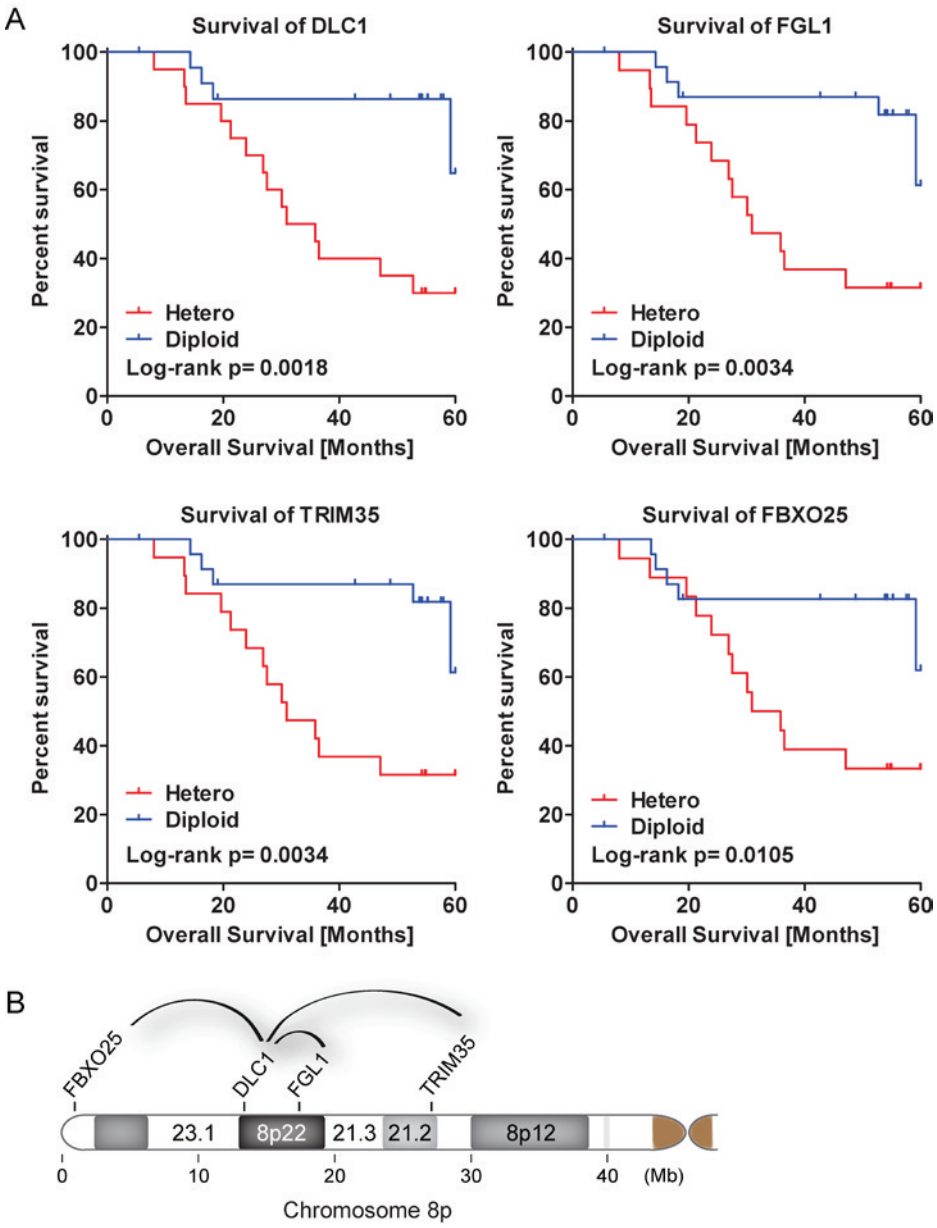

Fig. S6. Survival association of copy number loss of DLC1, FGL1, TRIM35 and FBXO25 in HCC patients. (*A*) Survival curves of HCC patients comparing copy number (diploid vs. heterozygous loss) for the indicated individual chromosome 8p genes. Statistical tests were performed as described (3). (*B*) Schematic illustration of the chromosome position of the validated HCC tumor suppressor genes showing cooperativity with DLC1.

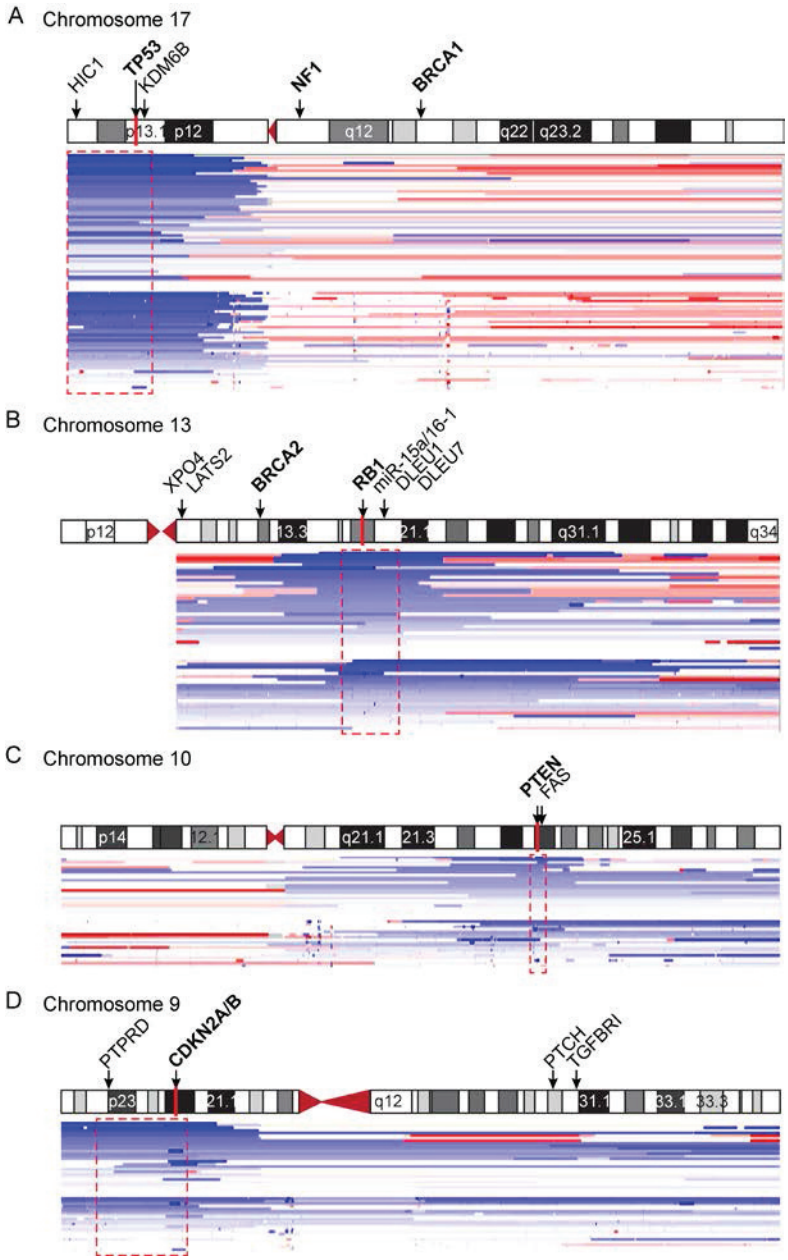

Fig. S7. Deletions at established TSG loci often include multiple candidate tumor suppressor genes. Schematic diagrams of human chromosomes 17 (*A*), 13 (*B*), 10 (*C*) and 9 (*D*), with deletions indicated in blue and amplifications indicated in red from individual HCCs (based on 140 samples) as in Fig. 1*A*. The location of the most established tumor suppressor on each chromosome (*TP53*, *RB1*, *PTEN*, and *CDKN2A/B*) is indicated as a red line on the chromosome, with other established or candidate tumor suppressor labeled in black. Red box highlights the most common deleted region.

Table S1. Gene names, chromosome location and deletion frequency of selected 8p candidate tumor suppressor genes outside 8p22.

	Gene Symbol	Cyto-band	Description	Start #	Stop #	Deletion frequency (%)
8p23	FBXO25	8p23.3	F-box protein 25	356808	419876	44.02
	ERICH1	8p23.3	glutamate-rich 1	614200	681226	43.54
	ARHGEF10	8p23	Rho guanine nucleotide exchange factor (GEF) 10	1772149	1906807	41.15
	CSMD1	8p23.2	CUB and Sushi multiple domains 1	2792875	4852328	41.63
	MCPH1	8	microcephalin 1	6264121	6506026	41.63
	ANGPT2	8p23.1	angiopoietin 2	6357172	6420784	41.63
	PINX1	8p23	PIN2-interacting protein 1	10622884	10697299	42.11
8p21-p11	LZTS1	8p22	leucine zipper, putative tumor suppressor 1	20103676	20112803	41.63
	BIN3	8	bridging integrator 3	22477931	22526661	44.02
	TNFRSF10B	8p22-p21	tumor necrosis factor receptor superfamily, member 10b	22877646	22926700	47.37
	LOXL2	8p21.3-p21.2	lysyl oxidase-like 2	23154410	23261722	46.41
	BNIP3L	8p21	BCL2/adenovirus E1B 19kDa interacting protein 3-like	26240523	26270644	44.02
	TRIM35	8	tripartite motif-containing 35	27142404	27168834	49.28
	CLU	8p21-p12	clusterin	27454451	27472327	47.85
	CCDC25	8	coiled-coil domain containing 25	27590833	27630170	46.41
	SCARA5	8	scavenger receptor class A, member 5 (putative)	27727736	27850198	46.41
	DUSP4	8p12-p11	dual specificity phosphatase 4	29193611	29208185	44.02
	NRG1	8	neuregulin 1	31497268	32622073	36.36
	SFRP1	8p12-p11.1	secreted frizzled-related protein 1	41119478	41166980	32.06

Selection criteria are schematically shown in Supplementary Fig. S1. DOK2, a recently reported 8p lung tumor suppressor (5) is not strongly underexpressed in HCC and thus is not within the candidate TSG list (see Fig. S1).

Table S2. Overview of the results from the pooled screening for 8p23, 8p21-11 TSGs listed as fold increase compared to the experimental control.

	Gene	fold increase compared to Control*	SEM (n=6)	p-value (t-test)	Penetrance (# of tumors/# of injection sites)
8p23	Fbxo25	25.15	+/- 6.00	0.220	6/6
	Erich1	2.63	+/- 1.91	0.420	2/6
	Arhgef10	28.9	+/- 5.10	0.047	5/6
	Csmd1	7.36	+/- 3.03	0.110	3/6
	Mcph1	1.08	+/- 0.55	0.890	2/6
	Angpt2	10.61	+/- 3.72	0.210	6/6
	Pinx1	8.0	+/- 2.80	0.120	4/6
8p21-p11	Lzts1	3.89	+/- 1.99	0.220	2/6
	Bin3	9.90	+/- 3.38	0.042	3/6
	Tnfrsf10b	11.6	+/- 3.30	0.140	4/6
	Loxl2	13.0	+/- 4.90	0.160	2/6
	Bnip3l	14.02	+/- 3.10	0.036	6/6
	Trim35	9.83	+/- 2.23	0.013	6/6
	Clu	0.82	+/- 0.76	0.150	1/6
	Ccdc25	1.28	+/- 1.04	0.720	6/6
	Scara5	8.3	+/- 2.40	0.043	4/6
	Dusp4	0.4	+/- 0.70	0.360	1/6
	Nrg1	2.4	+/- 1.30	0.230	4/6
	Sfrp1	0.77	+/- 1.24	0.840	1/6

***** fold increase was calculated to the corresponding experimental shControl at day 49 and day 42 for Bnip3l and Trim35

Table S3. Somatic mutations of 8p TSGs reported in databases or the literature.

Gene	COSMIC (1)	HGMD (2)	Literature
ARHGEF10	Colon: 1/33 S28L (Missense)		
BNIP3L	0/181		Ovarian cancer, 1/40 (Lai et al., Br J Cancer 2003)
DLC1	Kidney: 1/101; R347* (Nonsense) Lung: 1/12 ; K237N, R1294C (Missense) Pancreas: 1/2 R1425Q (Missense)		HCC, ovarian, colorectal and prostate (Wilson et al., Hum Mutat 2000; Park et al., Int J Oncol 2003; Liao et al., Cancer Res 2008)
FBXO25	Ovarian: ; 1/1; A347D (Missense)		
FGL1	0/44		
TNFRSF10B	0/605	Squamous cell carcinoma, head and neck (Insertion); Pai et al., Cancer Res 1998	Colorectal; truncating mutation (Macartney-Coxson et al., BMC Cancer 2008) Non-small cell lung cancer (Lee et al., Cancer Res 1999) Metastatic breast cancer (Shin et al., Cancer Res 2001)
TRIM35	0/180		
SCARA5	Melanoma: 1/1; E270K (Missense)		
VPS37A	0/44		

(1) www.sanger.ac.uk/genetics/CGP/cosmic/

(2) www.hgmd.cf.ac.uk/ac/index.php

Table S4. List of qRT-PCR primers.

mDlc1:	5'-CCACTGATATCCCGGAAAGA-3' and 5'-AAGCTGTGCCACCTCAGTCT-3'
mFgl1:	5´-GGAGGGGGATGGACTGTAAT-3' and 5´-GCCAGTATTCGCCATTGTTT-3'
mVps37a:	5´-TGCAAAGGCAACATGAACTC-3' and 5´-CGATTCTTCCTCAGCTTCGT-3'
mArhgef10:	5'-GAGATGCCGACCAGCGATG-3' and 5'-TCGTTGTAAACCGTCTCGATG-3'
mTnfrsf10b:	5'-CGGGCAGATCACTACACCC-3' and 5'-TGTTACTGGAACAAAGACAGCC-3'
mFbxo25:	5'-AAGGTGTGACCCCTGTAGC-3' and 5'-CCTCTTTTTGGCTGCGTATTCA-3'
mScara5:	5'-CATGGATTTCACAATGATTCGCC-3' and 5'-TCCCCGTCCTTCTTGTCCC-3'
mBnip3l:	5'-ATGTCTCACTTAGTCGAGCCG-3' and 5'-CTCATGCTGTGCATCCAGGA-3'
mTrim35:	5'-TTCCGGGCCAAGTGTAAGAAC-3' and 5'-CCAAGTCGTTTGCACCTCA-3'
mGapdh:	5'-GGTGAAGGTCGGTGTGAACG-3' and 5'-CTCGCTCCTGGAAGATGGTG-3'
mActin:	5´-CCACCGATCCACACAGAGTA-3´ and 5´-GGCTCCTAGCACCATGAAGA-3´

Supplementary References

1. Chen X*, et al.* (2002) Gene expression patterns in human liver cancers. *Molecular biology of the cell* 13(6):1929-1939.
2. Mas VR*, et al.* (2009) Genes involved in viral carcinogenesis and tumor initiation in hepatitis C virus-induced hepatocellular carcinoma. *Mol Med* 15(3-4):85-94.
3. Roessler S*, et al.* (2010) A unique metastasis gene signature enables prediction of tumor relapse in early-stage hepatocellular carcinoma patients. *Cancer research* 70(24):10202-10212.
4. Wurmbach E*, et al.* (2007) Genome-wide molecular profiles of HCV-induced dysplasia and hepatocellular carcinoma. *Hepatology* 45(4):938-947.
5. Berger AH*, et al.* (2010) Identification of DOK genes as lung tumor suppressors. *Nat Genet* 42(3):216-223.